# Frequent Mass Movements from Glacial and Lahar Terraces, Controlled by Both Hillslope Characteristics and Fluvial Erosion, are an Important Sediment Source to Puget Sound Rivers

**Daniel N. Scott[1], Brian D. Collins[1]**

[1]University of Washington, Department of Earth and Space Sciences, Seattle, WA

Corresponding author: Daniel N. Scott (scott93@uw.edu)

**Key Points:**

- Glacial and lahar terraces deliver sediment to Puget Sound Rivers primarily via frequent, small mass movements.
- Terrace sediment has a substantial coarse-grained fraction, is likely resistant to attrition, and is delivered low in river networks.
- Considerable spatial variation in size and frequency of mass movements is partly explained by hillslope geometry and failure mechanism.

---

This is a peer-reviewed, accepted version of a now-published manuscript at *Water Resources Research*. The published version has slightly different content and corrections to minor errors in this version, although none of the conclusions changed during review. Please see the final, accepted version of this manuscript at the "Peer-reviewed Publication DOI" link on this webpage. Please feel free to contact the corresponding author to request a pdf copy of the published version of this manuscript.



Full Citation:

Scott, D. N., Collins, B. D. (2021), Frequent Mass Movements from Glacial and Lahar Terraces, Controlled by Both Hillslope Characteristics and Fluvial Erosion, are an Important Sediment Source to Puget Sound Rivers, *Water Resources Research*, DOI: 10.1029/2020WR028389

---

## Abstract

Mass movements from glacial and lahar terraces in the middle and lower reaches of rivers draining the Washington Cascade Range to Puget Sound may represent a substantial but poorly quantified portion of those rivers' sediment supply and pose significant mass movement hazards. We used repeat LiDAR elevation data, aerial imagery, and well logs to quantify and characterize terrace sediment delivery in nine major watersheds over a median period of 12 years. In the 1946 river kilometers for which repeat LiDAR was available (71% of the 2736 total river kilometers flanked by terraces), 167 mass movements eroded 853,600 ± 19,400 $m^3$/yr. Analysis of mass movement frequency and volume indicates that terrace sediment delivery is dominated by small, frequent mass movements, as opposed to large, infrequent ones like the 2014 Oso landslide. This sediment source is low in river networks, well connected to streams, and has a substantial coarse-grained and durable component, all of which increase its significance to sedimentation in developed, lowland reaches. However, rates of terrace sediment delivery vary among basins and between adjacent terraces, which are stratigraphically laterally heterogeneous. While lateral fluvial erosion is usually necessary to initiate terrace mass movements, valley bottom geometry and terrace stratigraphy poorly predict erosion volume, which is better predicted by hillslope geometry and mass movement style. Effective management of sedimentation and mass movement hazard should acknowledge the importance of terrace sediment delivery and the variability among and within watersheds in sediment delivery, sediment characteristics, and failure mechanisms.

## Plain Language Summary

Extensive terraces, composed of sediments derived from past glaciations and volcanic mudflows, flank rivers in the Puget Sound region. Landsliding of these terraces creates local hazards but also delivers sediment to rivers which transport it downstream to developed, lowland areas, where sediment can build up and cause river migration and flooding hazards. Measurements of the land surface through time show that these terraces deliver large volumes of sediment to rivers that may have a significant effect on rivers downstream. In addition, small, frequent landslides deliver more sediment over time to rivers than large, infrequent ones. Examining how both river erosion and the composition and shape of these terraces influence the volume of sediment delivered by landslides to rivers shows that both factors contribute to determining landslide location and size. Effectively managing landslide and river hazards in the Puget Sound region requires a detailed understanding of terrace characteristics and the erosional patterns of their adjacent rivers.

## 1 Introduction

In paraglacial regions, expansive terraces can deliver substantial quantities of sediment to the middle and lowland reaches of river networks (Church and Slaymaker, 1989). This runs counter to the expectation that sediment delivery (i.e., transport of sediment from hillslopes to rivers) is greatest in headwaters (Schumm, 1977; Wohl, 2020), and disrupts the typical trend of downstream decreasing specific sediment yield (Ballantyne, 2002; Kovanen and Slaymaker, 2015; Slaymaker, 2003). Rivers draining to the Puget Sound exemplify this phenomenon. Steep bluffs incised by rivers to form glacial and lahar terraces (hereafter referred to simply as terraces; **Figure 1**) in this region are landslide prone (LaHusen et al., 2016) and constitute a paraglacial sediment source (Church and Ryder, 1972; Slaymaker, 2009); sediment production from Holocene lahar terraces is an analogous phenomenon, as both involve remobilization of relict sediment deposits from landforms in a "transitional" (Slaymaker, 2009) or "unstable" (Ballantyne, 2002) state of incomplete adjustment to climate and base level.

A large sediment influx near the Puget Sound lowland could disproportionately induce lowland channel response compared to sediment supplied from headwaters (Anderson and Jaeger, 2020; Collins et al., 2019): the coarse fraction of continental glacial deposits is composed primarily of resistant lithologies (Armstrong et al., 1965; Collins and Dunne, 1989) and, because of its origin low in the channel network, is subject to shorter transport distances and less potential for attrition. Deposition in these inherently aggradational lowland reaches (Collins and Montgomery, 2011) exacerbates hazards from lateral channel migration and flooding (Anderson and Jaeger, 2020; Collins et al., 2019; Stover and Montgomery, 2001). Additionally, understanding sediment supply and sediment transport dynamics, especially in rivers with major lowland sediment sources, is key to effectively restoring valley bottom habitat (Beechie et al., 2001; Benda et al., 1992) and predicting the effects of restoration strategies such as levee setback or Stage 0 restoration (Powers et al., 2019) that give rivers more freedom to reshape their valley bottoms. Although identified as an important sediment source in the nearby Fraser Lowland (Church and Slaymaker, 1989; Kovanen and Slaymaker, 2015), the quantitative importance, spatial distribution, sedimentologic characteristics, and delivery mechanisms of terrace sediment have yet to be systematically quantified in the Puget Sound region.

The first of this study's two primary objectives is to measure the spatial distribution, magnitude, and characteristics of terrace sediment delivery to Puget Sound rivers (Objective 1). This includes determining how much eroded sediment makes it to rivers over a given timescale (i.e., the lateral sediment connectivity (*sensu* Wohl et al., 2019) between terraces and rivers) and what fraction of the delivered volume is coarse enough to act as bed material load that can affect downstream channel morphology. Another aspect of terrace sediment delivery is the magnitude and frequency of mass movements that deliver sediment (Kovanen and Slaymaker, 2015; LaHusen et al., 2016; Perkins et al., 2017). The 2014 Oso landslide was only the latest in a Holocene history of large mass movements (Booth et al., 2017; LaHusen et al., 2016), which are widespread along Puget Sound rivers (Perkins et al., 2017). However, such large mass movements are less frequent than much smaller mass movements (e.g., Gardner et al., 2009; Radloff and Bunn, 2018). Here, we seek to determine if, over time, most terrace sediment enters rivers from infrequent, very large mass movements, or from frequent, smaller failures.

The substantial variability in size and frequency of terrace mass movements motivates the second major broad question of this study: what geomorphic processes determine the occurrence, size, and resulting flux of sediment from terrace mass movements (Objective 2)? Terrace mass movements are commonly associated with lateral fluvial erosion (e.g., Gardner et al., 2009;

Wartman et al., 2016), which implies that fluvial processes, hillslope (i.e., areas, including terraces, outside the modern, fluvially shaped valley bottom) processes, or some combination of the two may regulate terrace sediment delivery. Here, we conduct an extensive investigation into the relative importance of fluvial versus hillslope processes in regulating the occurrence and volume of terrace mass movements.

Several hypotheses guide this investigation. Terrace mass movement volume is likely a function of oversteepening by fluvial erosion and hillslope processes (LaHusen et al., 2016; Wartman et al., 2016). There is substantial variability in failure mechanisms (i.e., landslide types; Varnes, 1958) that occur along terrace bluffs (e.g., contrast Gardner et al., 2009; Wartman et al., 2016). This motivates us to hypothesize that failure mechanism and associated hillslope geometry (i.e., bluff height from the base to the top of the terrace on which the mass movement occurred, mass movement length from the upstream-most to downstream-most edge of the mass movement along flow, and bluff slope from the bluff top to base along steepest descent; Figure 1) correlate with mass movement volume (Hypothesis 1), which would imply that the processes that regulate failure mechanism (hillslope materials, hydrology, fluvial erosion rates) also control terrace mass movement volume. Fluvial incision is the primary driver of relief and oversteepening of terrace bluffs (LaHusen et al., 2016; Wartman et al., 2016), so we also hypothesize that lateral fluvial erosion into the base of terrace bluffs is necessary to initiate mass movements (Hypothesis 2a). If fluvial erosion is generally necessary for terrace mass movement, then it also stands to reason that more intense lateral fluvial erosion, such as may occur on steeper, more confined valley bottoms, should increase the frequency of terrace mass movements and deliver higher fluxes of terrace sediment to rivers (Hypothesis 2b). The presence of impermeable and low strength glaciolacustrine (Ql) sediment in terrace stratigraphy can cause elevated pore pressures and act as a low strength layer in terraces and has been proposed as a likely control on mass movement volume (Perkins et al., 2017). This implies that terrace mass movement volume should positively correlate with the proportion of Ql in terraces (Hypothesis 3). While stratigraphic position, or the number of layers, of Ql also likely regulates mass movement volume, we lacked the data to evaluate its importance in this work.


**Figure 1**. An actively eroding glacial terrace along the Skykomish River, at 47.841°, -121.657° facing west (terrace is "snohomish19" in Dataset S1). Inset shows detail of top of terrace. White vertical line shows bluff height. Diagonal green line shows bluff slope. Orange curve shows mass movement length.

## 2 Study Area

To address these objectives and hypotheses, we measured sediment delivery to valley bottoms from valley bottom-adjacent, terrace-forming sediment reservoirs along rivers draining from the west flank of the Cascade Range of Washington to Puget Sound (Figure 2). Glacial terraces formed by subglacial erosion of the regional fill of Pleistocene till, outwash, and glaciolacustrine sediments (Armstrong et al., 1965; Troost, 2016) during the late stages of the Vashon Glaciation (Booth, 1994) or by post-glacial fluvial incision into that fill driven by changes to base level and isostatic rebound (Dethier et al., 1995; Thorson, 1980). Lahar terraces formed from fluvial incision (e.g., Beechie et al., 2001) through extensive deposition of lahars from Glacier Peak in the Skagit (Dragovich et al., 2002a) and Stillaguamish basins (Dragovich et al., 2002b), Mt. Baker in the Skagit and Nooksack basins (Scott et al., 2020) and from Mt. Rainier in the Puyallup, Green, and Nisqually basins (Crandell, 1971; Vallance and Scott, 1997).

The nine river networks (Figure 2) drain from steep, formerly or presently glaciated alpine headwaters through confined mountain valleys into broader valleys carved into the Puget Sound lowland's glacial fill before reaching Puget Sound (Collins and Montgomery, 2011). Averaged across these basins, approximately 56% (range between 29 and 77%) of the stream length with a drainage area over 15 $km^2$, totaling 2736 river kilometers, has adjacent Pleistocene glacial and/or Holocene lahar terraces, generally located in the lower and middle portions of each basin (Figure 2).

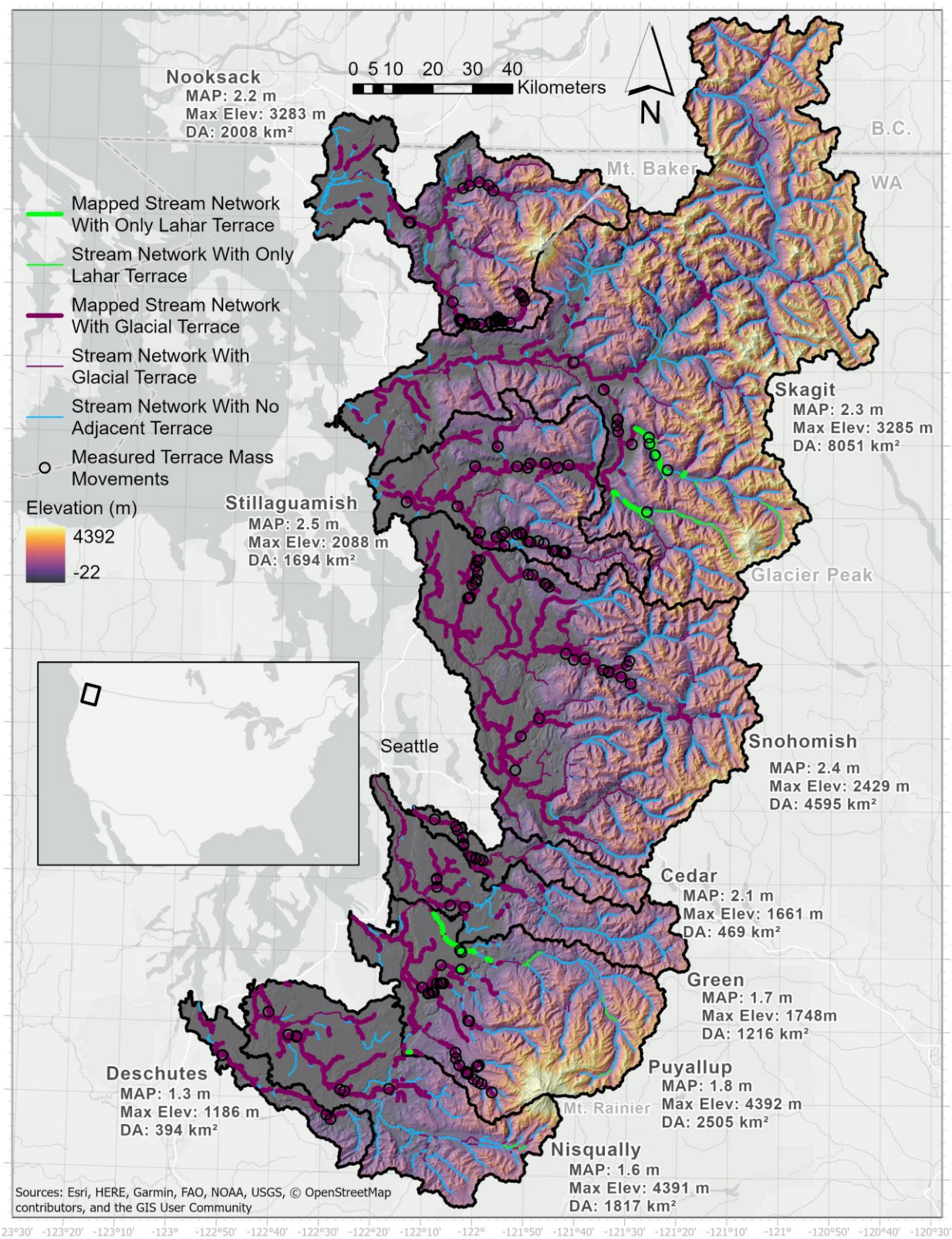


**Figure 2**. Map showing study basins, measured terrace mass movements, and stream networks in each basin. Steam networks (blue) are colored by the presence of glacial (dark purple) or lahar (light green) terraces adjacent to the valley bottom and whether the stream network with adjacent

terraces (i.e., in the terrace domain) had sufficient repeat LiDAR coverage to enable mapping and measuring terrace mass movement volumes (bolded). Inset shows map coverage (black rectangle). Mean annual precipitation (MAP; PRISM Climate Group, Oregon State University, 2012), maximum elevation (all basins drain to sea level with the exception of the Cedar, which drains to Lake Washington, just above sea level), and drainage area (DA) are listed for each basin. Note that for the Skagit and Nooksack basins, mean annual precipitation applies only to the portion of the basins within the United States.

## 3 Methods

### 3.1 Mapping and Measuring Terrace Mass Movements using LiDAR

To measure the volume of sediment eroded from glacial and lahar terraces (Objective 1), we constructed Digital Elevation Models (DEM) of Difference (DoD) using repeat LiDAR data. For each study basin, we collected all publicly available LiDAR datasets from 2002 to 2017, although the actual LiDAR-covered timespan varied between study basins from 6 to 14 years. We bilinearly resampled higher resolution DEMs to the lowest common resolution of the earliest LiDAR dataset, then subtracted earlier DEMs from later DEMs to obtain a DoD raster. We converted all DoD values less than ± 0.9 m (3 ft) to 0 to exclude values likely to be DEM noise as opposed to real elevation change. We used this thresholded DoD in conjunction with shaded relief representations of DEMs, aerial imagery, and a 1:100k scale geologic map of Washington State (Washington Division of Geology and Earth Resources, 2016) to identify and manually delineate polygons around the eroded area of terrace mass movements (i.e., excluding landslide deposits). Figure S1 shows examples of DoDs used to measure terrace mass movement volume (i.e., denuded volume). This use of repeat LiDAR DoDs to measure terrace erosion is inherently limited to the timespan of the LiDAR datasets used and does not represent material that may have been eroded outside the temporal span of this study. To estimate short-term (i.e., years) sediment connectivity, we noted whether each mass movement had a deposit at its base, in which case we considered it disconnected from the river, or had no deposit at its base, in which case we considered it to be connected to the river (i.e., the river had transported the material eroded from the terrace between LiDAR datasets).

To identify a patch of negative values in the DoD (i.e., erosion, or elevation loss) as a terrace mass movement, that patch needed to: 1) not appear to be the result of (i.e., not be adjacent to) human activities such as mining, grading, road-building, or urban development; 2) not erode alluvial fan deposits from tributaries, unless those fan deposits mantled thicker terrace deposits; and 3) erode or be adjacent to glacial sediment or lahar deposits with low-slope tops that do not exhibit morphologic evidence of modern fluvial reworking and exhibit a maximum terrace bluff height (see section 3.4) of at least 6.1 m (20 ft). We chose this height threshold based on observations of the boundaries between glacial and lahar terraces and modern, fluvial terraces mapped on 1:100 k and 1:24 k geologic maps, as well as our field experience working on rivers in the region, where alluvial banks can be as high as 6.1 m. A kernel density estimator fit to the distribution of maximum terrace heights in our dataset identified a distribution peak at 13.5 m, indicating that we likely excluded most or all active alluvial surfaces and included most or all glacial and lahar deposits (Figure S2).

We computed terrace mass movement volume by multiplying each DoD raster by its cell area, then summing the values of the resulting raster within the mapped extent of each mass movement. To estimate the measurement uncertainty in each volume estimate, we compiled the

LiDAR vertical root mean square (RMS) error for each DEM. Where LiDAR datasets had no reported vertical RMS error, we used the average vertical RMS error of all LiDAR datasets having a similar resolution and that reported a vertical RMS error. We then summed the vertical error for each pair of LiDAR datasets in quadrature to obtain a DoD RMS error, which we multiplied by the area of each mapped mass movement to obtain an uncertainty estimate for the eroded volume of each mass movement. We generally report terrace erosion as a volume per year, as most of the events we mapped appeared to occur in more than a single, noticeable event (59%, or 91 of the 154 that did not appear to fail continuously via ravel; Figure S3). To estimate the total terrace erosion measured within the mapped area of each basin, we conservatively summed maximum and minimum estimates using the high and low bounds, respectively, defined by the RMS error for each individual mass movement in each basin. Although these estimates represent only a short period of time (6 – 14 years), peak streamflows in this period were neither abnormally high nor low compared to peak streamflows in the historical flow record (Figure S4).

### 3.2 Delineating Terrace Spatial Distribution Along River Networks

To quantify the spatial distribution of terraces and potential terrace sediment delivery in each basin (Objective 1), we used 1:100 k-scale geologic maps (Washington Division of Geology and Earth Resources, 2016) and 10- to 30-m resolution DEMs to delineate the portions of channel networks having stream-lateral glacial or lahar terraces, which we refer to as the "terrace domain" (thin and bold green and purple lines in Figure 2), as well as the stream length along which active channels were in contact with and possibly eroding the base of terrace bluffs (not shown in Figure 2). We only examined the portions of stream networks with drainage area over 15 $km^2$ (all green, purple, and blue lines in Figure 2). This threshold included tributaries that had incised deeply enough through mainstem terraces to initiate mass movement but excluded incised, gully-like channels cutting through terraces that are otherwise being eroded primarily by larger streams. We then further delineated the proportion of the terrace domain covered by repeat LiDAR DEM data, which represents the proportion along which we were able to map terrace mass movements (bold green and purple lines in Figure 2; approximately 71% of the total stream network length in the terrace domain across all basins).

To determine the location distribution of terrace mass movements along the stream networks studied, we computed normalized drainage area at individual mass movements by dividing the drainage area at the mass movement by the entire basin area. We also normalized the valley bottom elevation at each mass movement by dividing it by the elevation of the highest point of the stream network with a drainage area over 15 $km^2$.

### 3.3 Determining Glacial Terrace Stratigraphic Characteristics

We used the Washington Department of Ecology Well Log Database (Washington State Department of Ecology, 2020) to characterize subsurface stratigraphy and qualitatively describe grain size of terraces, including the occurrence of Ql, which Perkins et al. (2017) suggested can be a primary control on the eroded volume of mass movements (Objective 1, Hypothesis 3). For each mapped mass movement, we consulted all well logs inferred to be from the same terrace as the mass movement. We then chose the one that likely represented the largest amount of the total height of the terrace and, if it was not the closest well log to the mass movement, was similar to the stratigraphy recorded in the closest well log. For that well log, we recorded the top depth and thickness of each layer likely to be Ql (i.e., dominantly silt or clay, although irregular log descriptions made this determination difficult and subjective). Finally, we computed the total

thickness of likely Ql layers for the portion of the core that intersected the elevation range of the mapped mass movement. Well logs were available to make this determination for 55 of the 167 mass movements that we mapped. We verified stratigraphic measurements qualitatively during field reconnaissance of select mass movements (Text S1).

### 3.4 Measuring Terrace Mass Movement Characteristics

To evaluate potential controls on mass movement volume (Objective 2, Hypotheses 1 – 3), we measured bluff geometric characteristics using the most recent LiDAR DEM for each mass movement. We measured failure length approximately parallel to the adjacent stream and bluff height from the stream or depositional zone to the top of the terrace as an average of three measurements along the feature's length. We also estimated bluff slope by measuring the horizontal width along steepest descent of each mass movement at the same three locations as bluff height, then dividing mean bluff height by mean width. We used the most recent DEM to measure total bankfull width of active channels and floodplain width, including the portion on which the channel could potentially migrate in the absence of anthropogenic constraints. We used the FluvialCorridor toolbox (Roux et al., 2015) and a 10 m DEM (30 m for the Nooksack and Skagit basins, which lack full 10 m DEM coverage) to record channel slope, mean elevation, and drainage area for the 500 m stream segment closest to each mass movement. We also noted whether the stream contacted the terrace bluff base, which we took to indicate direct delivery of sediment to the stream. For the few mass movements that were not adjacent to active channels, we used historical aerial imagery and King County (King County, 2020) and Army Corp of Engineers (United States Army Corp of Engineers, 2020) levee and revetment databases to determine whether those mass movements are artificially isolated from active channels by levees or revetments.

We used all Google Earth imagery available within the period defined by the two sets of LiDAR to determine the minimum number of times a terrace bluff face appeared to fail within that period. We interpreted substantial change to the terrace face texture or vegetation or visual evidence of terrace top edge retreat as evidence of failure. From this, we calculated a minimum rate of failures per year for each mapped mass movement.

To determine whether failure mechanism and hillslope geometry control mass movement volume (Hypothesis 1), we used LiDAR and Google Earth imagery to classify failures by mechanism using a description of landslide typology (Hungr et al., 2014; Varnes, 1958) modified to accommodate fluvially-induced mass movements. We verified this classification during field reconnaissance of select mass movements (Text S1). From Google Earth aerial imagery and LiDAR DEMs, we described failures as being either: (1) flows or slides, with clear evidence of fluidized mass movement (channelization, long runouts, no visible slip surface, entirely toppled vegetation) or movement along a defined shear plane (no channelization, visible intact blocks possibly with intact vegetation, noticeable slump block cracks); (2) outer bend lateral retreats, which displayed simultaneous fluvial lateral migration along an outer bend and terrace bluff face retreat on a relatively steep face with minimal runout; (3) outer bend falls, which showed little noticeable lateral retreat or bluff retreat despite changes to the bluff face appearance through time, likely indicating very frequent falls of material; or (4) complex failures that exhibited characteristics of both flows or slides as well as outer bend lateral retreat. Figure S5 shows examples of each failure mechanism.

### 3.5 Statistical Analyses

To test our hypotheses, we used a combination of multiple comparisons and evaluations of monotonic trends. To compare groups of data, we compared estimates of central tendency with 95% confidence intervals and used boxplots for visual analysis. To evaluate correlations between data, we used Spearman rank-sum correlation coefficients ($\rho$) and associated 95% confidence intervals (Bishara and Hittner, 2017), which nonparametrically determine the presence of a monotonic correlation (values near 1 or -1 indicate a near-monotonic, positive or negative correlation, respectively and values near 0 indicate no correlation). All statistical analyses were performed in the RStudio (RStudio Team, 2016) interactive development environment for R (R Core Team, 2018) using the car (Fox and Weisberg, 2019), asbio (Aho, 2019), and tidyverse (Wickham et al., 2019) packages. Figures were produced using ggplot2 (Wickham, 2016), cowplot (Wilke, 2019), and EnvStats (Millard, 2013) packages. All uncertainties reported indicate 95% confidence intervals unless otherwise defined.

## 4 Results and Discussion

### 4.1 Magnitude, Spatial Distribution, Frequency, and Characteristics of Terrace Erosion (Objective 1)

The importance of terrace erosion as a sediment source to Puget Sound rivers is a function of: 1) the volume of sediment eroded from terraces; 2) sediment connectivity between terraces and rivers, represented by the proportion of the volume eroded from terraces that is subsequently transported by fluvial erosion over short timescales (i.e., years); and 3) the grain size distribution and lithology of terrace sediment, because of their control on rate of attrition in fluvial transport, which together determine the degree to which terrace sediment may act as bed material load that can alter river morphology, especially in lowland reaches. We examine each of these in the three following sections.

#### 4.1.1 Terrace Sediment Eroded Volume

Terrace failures in our period of examination (2002 - 2017, 6 - 14 year timespan) eroded 853,600 ± 19,400 $m^3$/yr, corresponding to 3,500 ± 100 $m^3$/yr/km in the repeat LiDAR mapped portion of the terrace domain (71% of the total stream length in the terrace domain). Excluding the 2014 Oso landslide, which eroded 359,000 ± 3,400 $m^3$/yr, or 42% of the total across all nine basins, those values are 494,300 ± 16,100 $m^3$/yr and 2,100 ± 100 $m^3$/yr/km, respectively. Total eroded volume and eroded volume normalized by river kilometer vary among basins, the latter varying by a factor of 27, or a factor of 99 if the 2014 Oso landslide is included (Figure 3). Lahar sediments account for a substantial portion of the totals in only the Puyallup and Skagit River basins (4% and 19%, respectively) and a small portion (54 km, or 2.8%) of the total LiDAR mapped river length in the terrace domain.

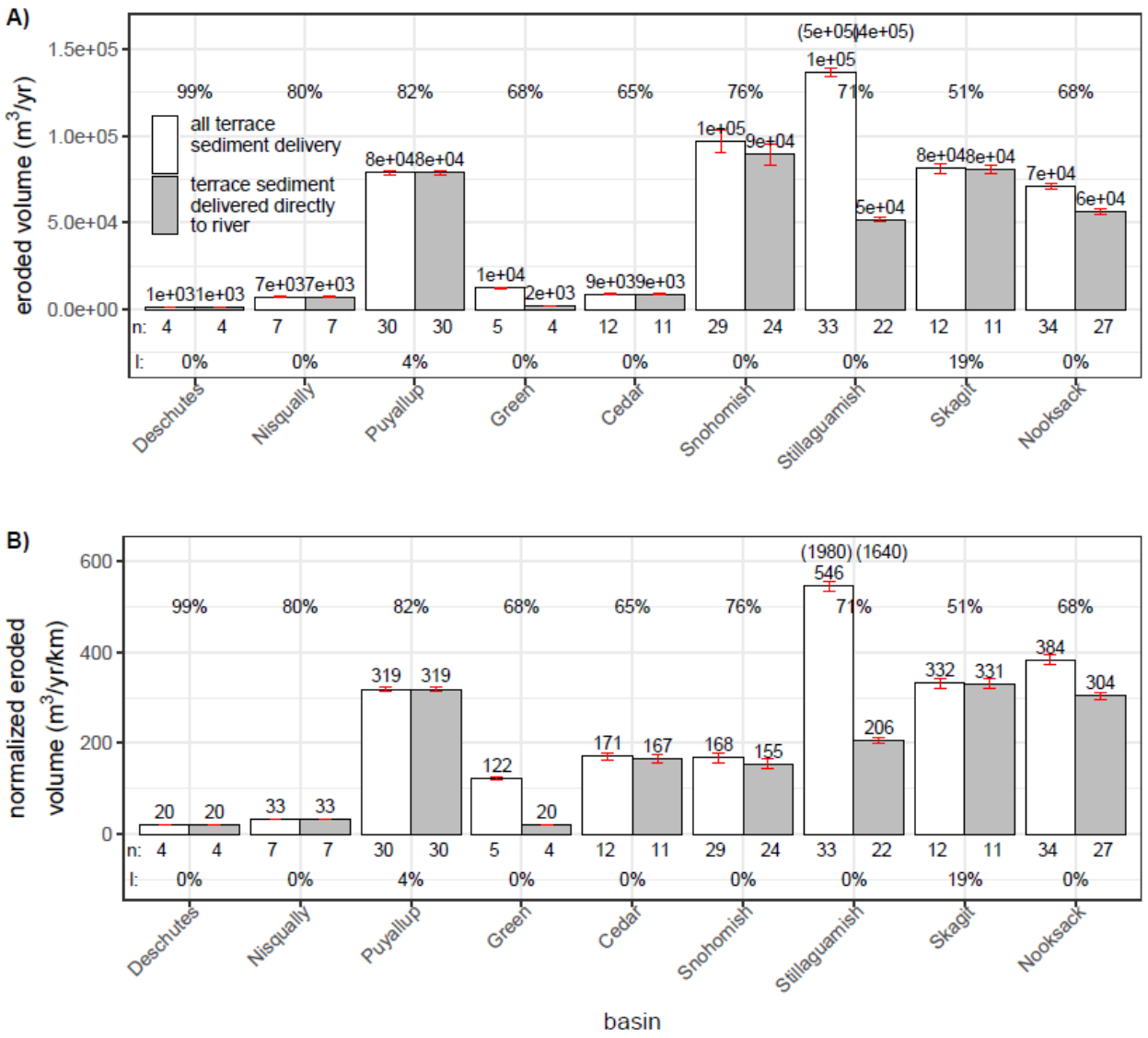


**Figure 3**. Bar plots showing the volume of terrace sediment eroded during the period of examination for each basin examined: (A) normalized by the period between repeat LiDAR datasets used to compute eroded volume and (B) normalized by repeat LiDAR mapped stream network length in the terrace domain (bold and purple lines in Figure 2). Values above bars show the value of each bar. Percentages above bars for each basin show the percent of the repeat LiDAR mapped stream network length in the terrace domain. Grey bars show only the mass movements denoted as being connected to the river over a short timescale (see sections 3.1 and 4.1.2). Red error bars represent uncertainty due to measurement error. Values in parentheses above the bars for the Stillaguamish basin represent the values including the 2014 Oso landslide. At the base of each plot, "n" shows the number of mapped erosion events for each bar and "l" shows the percent of the eroded volume sourced from lahar terraces.

### 4.1.2 Sediment Transport Connectivity Between Terraces and Adjacent Rivers

Nearly all the terrace mass movements that we mapped delivered sediment directly to adjacent rivers or form deposits that are rapidly eroded by rivers, indicating a high degree of

lateral sediment connectivity between terraces and rivers. Of the 167 mapped mass movements, 141 (84%; gray bars in Figure 3) appeared to deliver sediment directly to rivers (i.e., had no remaining deposit outside the channel in the latter LiDAR DEM), although that sediment may not be transported downstream immediately. Of the remaining 26 mass movements that did not deliver sediment directly to rivers, 22 showed evidence of fluvial erosion, and most of these had been largely eroded by the river at the time of our mapping. Only four (three in the Stillaguamish and one in the Snohomish, totaling 6,100 ± 300 $m^3$/yr, or approximately 1% of the non-Oso terrace erosion we mapped) had deposits that were entirely untouched by fluvial erosion, two of which were isolated from the river by revetments or levees. In contrast to the small landslides we mapped, which exhibited high sediment connectivity to adjacent rivers, large landslides such as the 2014 Oso Landslide tend to leave uneroded deposits for decades to millennia (LaHusen et al., 2016).

#### 4.1.3 Spatial Distribution of Pleistocene Glacial and Lahar Terrace Sediment Delivery Along River Networks

Terrace erosion is concentrated at low normalized elevations (Figure 4) because incised, oversteepened terraces are more common farther downstream in the study basins (Figure 2). This is especially true of four elongate basins characterized by mainstems that are much larger than their small tributaries, which contrast with the five basins characterized by large tributaries and a more equant shape (Figure S8). In equant basins, sediment is sourced from terraces along large tributaries, whereas in elongate basins, sediment is sourced from terraces along mainstems, presumably due to the lack of large, erosive tributaries. This difference in basin shape also results in differences in where in the drainage basin terrace erosion is located, despite the fact that most terrace sediment is delivered at low elevations in all basins: in equant basins, mass movements deliver more sediment at low normalized drainage areas (i.e., in tributaries in or near the lowlands). In contrast, in elongate basins, mass movements deliver more sediment at high normalized drainage areas (i.e., along the mainstem, although still within the lowlands; Figure 4).

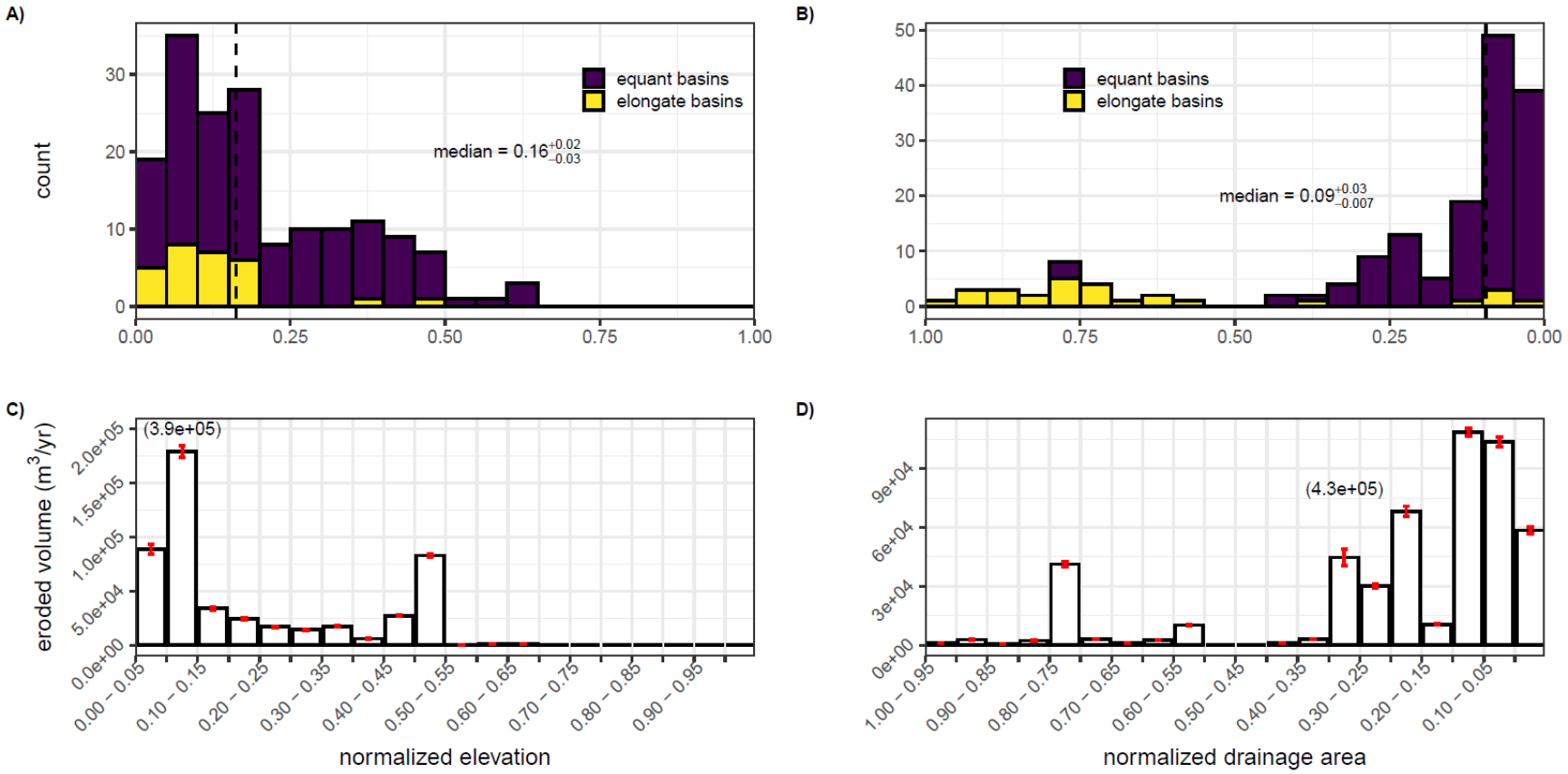


**Figure 4.** Spatial distribution of mapped terrace mass movements by frequency (A and B), and by total eroded volume (C and D), binned by normalized elevation (the elevation of the stream adjacent to the mass movement divided by the maximum elevation of the stream network with over 15 km$^2$ drainage area in the basin; A and C) and normalized drainage area (the drainage area of the stream adjacent to the mass movement divided by the basin drainage area; B and D). Note that the x axis is reversed for plots B and D, as low normalized elevations tend to correspond to high normalized drainage areas. For histograms (A and B) the vertical dashed line shows the median value. In C and D, red error bars represent measurement uncertainty, and values in parentheses indicate the value including the 2014 Oso landslide. Note the differing y axes. Equant basins include the Nooksack, Puyallup, Skagit, Snohomish, and Stillaguamish, and elongate basins include the Cedar, Deschutes, Green, and Nisqually.

### 4.1.4 Comparing Sediment Delivery from Small, Frequent Terrace Mass Movements with Larger, Infrequent Mass Movements

Our dataset includes primarily small mass movements (median eroded volume per terrace mass movement of $1146^{+190}_{-201}$ $m^3$/yr; Figure 5A) that occurred over a short period of 6 – 14 years (median of 12 years; Figure 5B). However, the 2014 Oso landslide, with an eroded volume 315 times the median volume of all other mass movements, contributed $42.1^{+0.6}_{-0.6}$ % of annualized terrace erosion during the period we examined. This raises the question of whether, over long periods of time, frequent, small failures or rare, large failures account for more total terrace erosion.

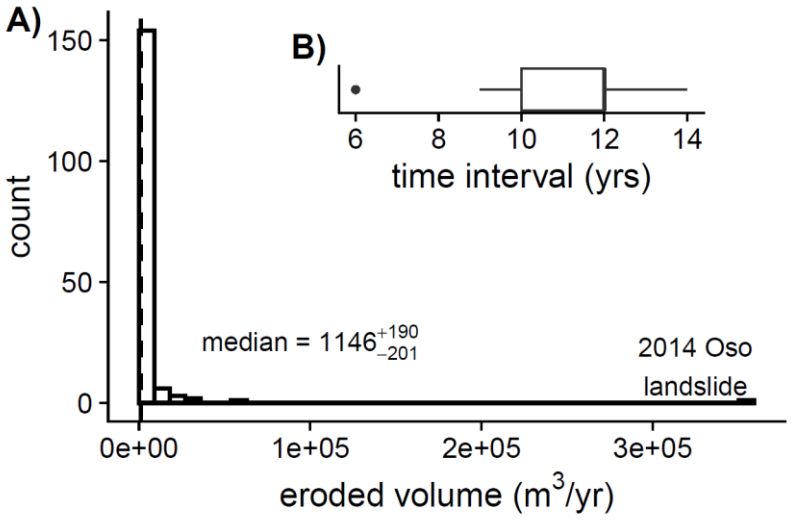


**Figure 5**. (A) Histogram of terrace erosion volume and (B) inset boxplot showing the time interval over which terrace erosion volume was measured by LiDAR differencing. Vertical dashed line shows median eroded volume exclusive of the 2014 Oso landslide, which is also given with 95% confidence interval uncertainty. Each histogram bin covers a span of approximately 8900 $m^3$/yr. For inset boxplot, bold vertical line represents the median (also the 75$^{th}$ percentile, in this case), box edges represent the first (25$^{th}$ percentile) and third (75$^{th}$ percentile) quartiles, and ends of horizontal lines represent 1.5 times the interquartile range. Solid black circle represents an outlier (outside of 1.5 times the interquartile range). Sample size for both plots is 167.

To address this question, we use as a recurrence interval for large mass movements the dated record of large failures from terraces in the North Fork Stillaguamish River over the last 2000 years. This record indicates a frequency of one event every 140 years (LaHusen et al., 2016). This recurrence interval from a single stream valley may not represent all Puget Sound basins and may be higher than the mean recurrence interval in the post-glacial period, as landslide frequency may have increased through time (Booth et al., 2017). Large, infrequent landslides can erode between 5,000,000 $m^3$ (our estimate for the 2014 Oso landslide, which is less than the approximately 8,000,000 $m^3$ estimate of Iverson et al., (2015) due to their use of more detailed failure plane modeling and our more conservative measurement of only denudation) and 35,000,000 $m^3$ (estimate by Iverson et al. (2015) for the nearby Rowan landslide) of sediment. Dividing the minimum and maximum values (5,000,000 and 35,000,000

$m^3$, respectively) by the estimated recurrence interval of 140 years, we estimate that large, infrequent landslides erode 143,000 ± 107,000 $m^3$/yr of terrace sediment. This is likely an overestimate, as the recurrence interval computed by La Husen et al. (2016) also includes landslides smaller than the 2014 Oso landslide. By comparison, the 166 small mass movements in the short (median 12 years) period of our study produced 494,300 ± 16,100 $m^3$/yr, which is much more than the amount produced by large, infrequent events as estimated above. In addition, the small landslides that make up the majority of our dataset tend to be far more laterally connected to rivers over short timescales, whereas large, infrequent landslides such as the Oso and Rowan landslides tend to only deliver a portion of their sediment to rivers over even millennial timescales (LaHusen et al., 2016). This implies that small, frequent landslides not only erode more terrace sediment over time but also contribute eroded sediment to rivers more immediately than do large, infrequent landslides.

#### 4.1.5 Importance of Terrace Erosion to Puget Sound Rivers

That terrace mass movements cumulatively erode substantial volumes of sediment and rivers rapidly erode nearly all that sediment suggests that terrace sediment could be an important sediment source to Puget Sound rivers. Comparing our estimates of terrace erosion to published sediment load data confirms this inference, although terrace erosion may be a more significant contributor to the sediment load of rivers draining currently unglaciated basins than to rivers draining currently glaciated basins. Our estimated eroded volume from terraces, extrapolated to the entirety of the terrace domain in each basin (i.e., values in Figure 3B divided by the proportion of the terrace domain we were able to map in repeat LiDAR for each basin), is 12 to 24 % of the magnitude of published sediment yields for glaciated basins and 12 to over 100 % of the magnitude of measured sediment yields for non-glaciated basins (Table 1). The substantial variability in this proportion for non-glaciated basins comes primarily from the Cedar River, where basin sediment yield is only estimated as bed material load, and hence is likely far lower than the total or suspended load of the basin. However, a previous investigation concluded that most of the Cedar River's coarse sediment yield comes from terrace erosion (Perkins Geosciences and Harper Houf Righellis, Inc., 2002).

**Table** 1.Comparison of published basin sediment yields to estimated terrace sediment erosion from this study. Percentages of basin-wide sediment yield reported here are given as a proxy for the relative importance of terrace sediment erosion in each basin, which cannot be compared directly to sediment yield.

| **Basin** | **Sediment yield ($m^3$/yr)[1]** | **Sediment yield type** | **Terrace erosion ($m^3$/yr)** | **Terrace erosion as percent of sediment yield** |
|---|---|---|---|---|
| Glaciated | | | | |
| Nooksack | 440,000 [2] | total load | 104,500 | 24% |
| Skagit | 1,275,000 [3] | total load | 159,000 | 12% |
| Puyallup | 430,000 [4] | suspended load | 96,000 | 22% |
| Nisqually | 50,000 [5] | suspended load | 9,100 | 18% |
| Not glaciated | | | | |
| | 640,000 [6] | suspended load | 192,600 | 30% |
| Stillaguamish | | | | |
| Snohomish | 250,000 [7] | suspended load | 127,400 | 51% |
| Cedar | 6,000 [8] | bed material load | 13,600 | 226% |
| Green | 53,000 [9] | suspended load | 18,000 | 34% |
| Deschutes | 13,000 [10] | suspended load | 1,500 | 12% |

[1]We use a bulk density of 2 tonnes/$m^3$ to convert sediment yield estimates (typically reported in tonnes/yr) to units comparable to mass movement volume estimates (Collins et al., 2019; Savage et al., 2000). [2]Anderson et al. (2019). [3]Curran et al. (2016b). [4]Czuba et al. (2012). [5]Curran et al. (2016a). [6]Anderson et al. (2017). [7]Nelson (1971). [8]Northwest Hydraulic Consultants, Inc. (2018). [9]Senter et al. (2018). [10]Nelson (1974).

Well log data and our field observations indicate that terraces likely contain high proportions of sand and coarser sediment, making terrace sediments important contributors to coarse bed material load and therefore downstream morphodynamics. Well logs covering the full height of the terrace mass movements we mapped (28 of the 55 records we examined) indicate that, on average, 50 ± 14 % by volume of the material delivered from mapped terrace mass movements is coarse, non-Ql sediment. This inference from well log data is limited, however, by the likely variability in the coarse fraction of terrace sediment among basins. Our field observations of actively eroding terraces (Text S1; Figures S6 and S7) indicate that terraces contain substantial amounts of coarse sediment and that exposed terrace stratigraphy agrees with well log descriptions and is strongly laterally heterogeneous, varying over distances as small as a few dozen meters. This makes the uncertainty on our coarse fraction estimate likely a lower bound on actual uncertainty. Our estimate is consistent with previous estimates of terrace gravel proportions in Cedar River terrace faces (range 0 to 100 %, median 35 %; Perkins Geosciences and Harper Houf Righellis, Inc., 2002). We lack sufficient well log data to estimate sediment size for lahar terraces, but previous sedimentologic investigations of Osceola Mudflow terraces in the headwaters of the Puyallup suggest they may contain 82 ± 3 % (Crandell, 1971) and 84 ± 2 % (Vallance and Scott, 1997) sand or coarser material. However, similar to glacial terraces, lahar terraces are likely laterally heterogeneous (Gomez and Lavigne, 2010).

The position of terrace sediment sources low in drainage basins (Figure 4) likely also increases the relative importance of terrace sediments to basin yield and to sedimentation in lowland reaches because lower travel distances would result in less attrition and loss to the washload (e.g., O'Connor et al., 2014). Puget Sound terrace sediment is primarily continental glacial drift which is dominated by resistant metamorphic and igneous rocks (Armstrong et al., 1965), and similar continental outwash in the nearby, southern Olympic Peninsula Satsop River basin is resistant to attrition (Collins and Dunne, 1989). The limited data reported here indicate that because terrace sediments have a substantial fraction of sediment coarser than silt dominated by relatively resistant lithologies and enter rivers low in the drainage basin and thus undergo shorter travel distances, their role in effecting morphologic change in lowland reaches may be large relative to sediment delivery from distant glaciated headwaters. This finding motivates more in-depth analysis of sediment attrition rates to quantify the relative contributions of various sediment sources to downstream sedimentation. It also motivates more examinations of the efficiency with which rivers can transport delivered sediment (e.g., Anderson et al., 2019; Anderson and Konrad, 2019).

Unlike many drainage basins, where sediment is sourced mostly from the headwaters, Puget Sound rivers have substantial sediment supply from paraglacial sources in the middle and lower reaches of drainage basins, very close to depositional zones. This is similar to the paraglacial Fraser Lowland (Kovanen and Slaymaker, 2015) but contrasts to the La Sueur River, Minnesota, USA where sediments are sourced from glacial bluffs, triggered by a post-glacial, upstream-progressing headcut, in the middle to headwater reaches (Gran et al., 2013). The supply of coarse, resistant sediment from terraces low in river networks, much of it from frequently occurring mass movements, highlights the potential importance of paraglacial and, in some basins, "paravolcanic" sediment sources in regulating the sediment dynamics and channel morphodynamics of Puget Sound rivers, especially in developed, lowland reaches.

### 4.2 Geomorphic Controls on Pleistocene Glacial and Lahar Terrace Erosion (Objective 2, Hypotheses 1-3)

#### 4.2.1 Influence of Failure Mechanism on Mass Movement Volume (Hypothesis 1)

The styles, or failure mechanisms, of terrace mass movements vary in their geometry, as defined by stream-parallel mass movement length, terrace bluff height, and bluff slope (Figure 6A-C). In general, flows/slides tend to be channelized and thus have small stream-parallel lengths (Figure 6A); occur on taller bluffs (Figure 6B), which may fail less frequently via slumping or ravel compared to shorter bluffs; and have relatively low-angle failure planes (Figure 6C) compared to other failure mechanisms. Outer bend falls tend to occur only on steep bluffs (Figure 6C) formed in cohesive materials and to fail continuously (e.g., we observed continual delivery of gravel from the especially coarse outer bend falls along the Cedar River; Figure S7) as opposed to failing episodically. Outer bend lateral retreat, the most common failure type, accounting for 56 %, or 93 of 166 mapped features (Figure 6D), tends to occur on short bluffs (Figure 6C), likely by a process similar to slump-failure of stream banks (e.g., Klösch et al., 2015). Tall bluffs that are likely comprised of heterogeneous or otherwise poorly cohesive material tend to fail via a combination of the outer bend lateral retreat and flow/slide mechanisms, and in most of these types of failures, we observed outer bend lateral retreat to only affect the lower portion of bluff faces, whereas the flow/slide portion usually extended above the scour of the outer bend lateral retreat.

These geometric differences among failure mechanisms result in substantial differences in eroded volume (Figure 6D). Flow/slide and outer bend lateral retreat failures tend to have similar annually normalized volumes. Outer bend falls, despite their tendency to fail almost continuously, deliver the least annually normalized volume. Compound failures consisting of outer bend lateral retreat combined with flow/slides deliver significantly more material than outer bend lateral retreat or flow/slides alone.

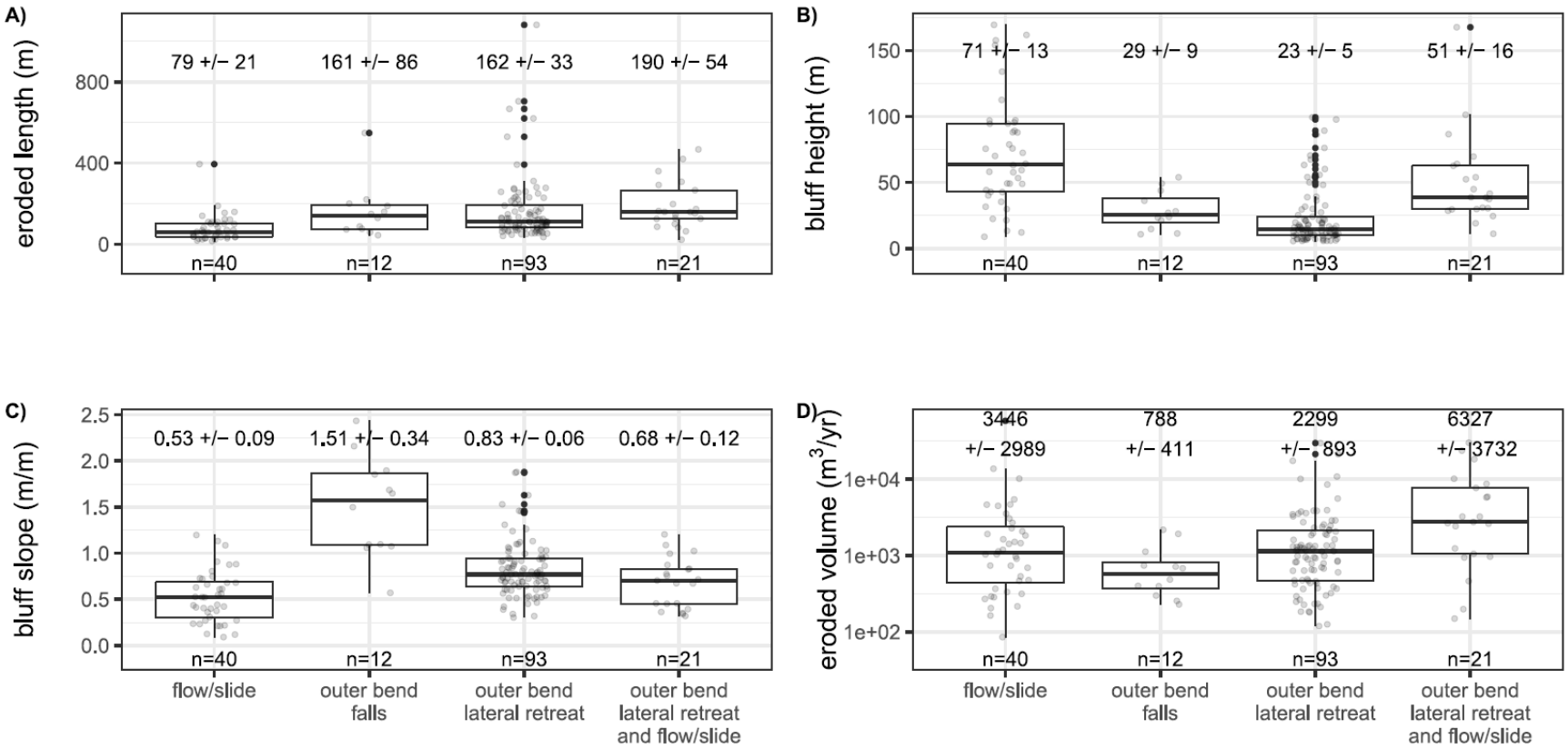


**Figure 6**. Boxplots showing: (A) differences among failures mechanisms and the stream-parallel length of each measured landslide, (B) the mean height of the bluff on which landslides occurred, (C) the slope of the resulting failure plane following landsliding, and (D) the volume eroded by each landslide (note the logarithmic y-axis). Bold horizontal lines represent the median, box edges represent the first (25$^{th}$ percentile) and third (75$^{th}$ percentile) quartiles, and ends of vertical lines represent 1.5 times the interquartile range. Solid black circles represent outliers (outside of 1.5 times the interquartile range), and transparent gray circles with arbitrary x-axis scatter within each category show all data. The mean of each group and associated 95% confidence interval uncertainty are shown above each box. Note that these analyses and this figure exclude the 2014 Oso landslide, as it is a single, infrequent, and much larger event than the ones shown here and would skew our estimates of these central tendencies.

### 4.2.2 The Role of Fluvial Erosion in Priming Terrace Mass Movements (Hypothesis 2)

If lateral fluvial erosion is necessary to initiate terrace mass movements, we would expect that most mass movements would occur when the adjacent river is actively eroding the base of a terrace bluff. Indeed, 89%, or 141 of the 167 mapped mass movements, occurred while the river was immediately adjacent to, and presumably eroding, the terrace base; exposed, actively eroding banks observed in aerial imagery for most of these mass movements support this assumption. However, active lateral fluvial erosion is not consistently sufficient to initiate failure: the degree to which streams contact terraces does not correlate to terrace erosion volume or mass movement frequency. This lack of correlation implies that while fluvial lateral erosion is the dominant trigger of terrace mass movements, many are still triggered by hillslope processes (e.g., elevated pore water pressures due to rainfall).

Whereas fluvial lateral migration primes terraces for eventual mass movement, it is likely insufficient on its own to regulate their volume. We found no correlation between basin-wide annual terrace erosion volumes ($\rho = 0.18^{+0.58}_{-0.74}$, n = 9) or the number of terrace mass movements per repeat LiDAR mapped river km in the terrace domain ($\rho = -0.15^{+0.74}_{-0.59}$, n = 9) and the proportion of the stream network that we mapped in LiDAR as contacting terraces. Similarly, steeper and more laterally confined valley bottoms, which might be expected to have more frequent contact between the stream and adjacent terraces, don't tend to produce higher rates of terrace sediment erosion: We found no correlation between channel slope ($\rho = -0.11^{+0.16}_{-0.37}$, n = 166) or the ratio of valley bottom width to channel width (i.e., confinement, $\rho = -0.02^{+0.16}_{-0.16}$, n = 166) and the rate of terrace erosion.

### 4.2.3 The Role of Glaciolacustrine Sediment in Regulating the Magnitude of Sediment Delivery from Terraces (Hypothesis 3)

Perkins et al. (2017) hypothesize that terraces with greater proportions of Ql have a greater incidence of large mass movements due to Ql effects on hydrology and material strength. However, we found only a weak correlation between the proportion of Ql and the volume of material eroded from studied terraces (Figure 7A). Terraces with higher proportions of Ql deliver marginally more sediment per individual failure, as opposed to more frequently failing (Figure 7B shows no correlation between mass movement frequency and Ql proportion) or failing by mechanisms that tend to deliver more sediment per event (we found no significant difference in Ql between failure mechanisms).

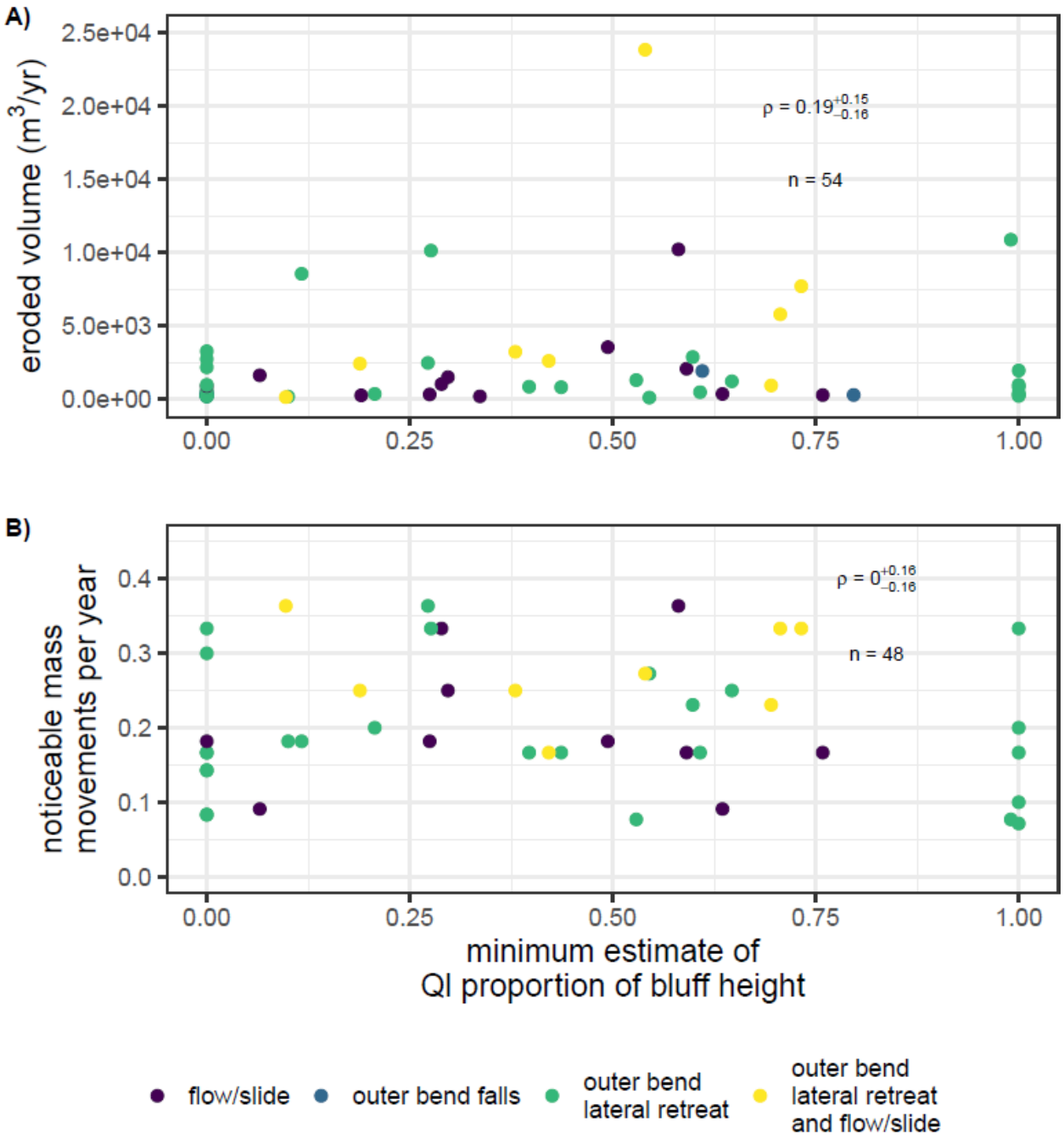


**Figure 7**. Scatterplots showing: (A) the relationship between the ratio of Ql thickness to total bluff height versus the annual eroded volume for each landslide and (B) the frequency of noticeable failures. Data are colored by failure mechanism. Spearman correlation coefficient (ρ), 95% confidence interval on ρ, and sample size (n) are shown on each plot. Note that outer bend falls are not shown on plot B because we could not reliably distinguish individual failures.

#### 4.2.4 Synthesis of Controls on Terrace Mass Movement Volume

Mass movement volume correlates with failure mechanism, which in turn correlates with hillslope geometry, supporting our Hypothesis 1. This contrasts with previous work that found

that terrace bluff geometry does not correlate with mass movement volume (Kessler et al., 2013), although bluff erosion in that study was largely due to undercutting, seepage, piping, and freeze/thaw, which may play lesser roles in the taller bluffs examined in this study. Over half of the mass movements we mapped were due to outer bend lateral retreat, indicating a strong component of fluvial lateral erosion in triggering terrace sediment delivery. The mechanism of fluvial lateral erosion oversteepening bluffs and triggering mass movements is conceptually similar to bank slump erosion, in which bank materials and hillslope processes regulate failure mechanism and resulting mass movement volume and hazard (Klösch et al., 2015).

Both hillslope characteristics and lateral fluvial erosion play a role in regulating terrace mass movement volume. That most mapped mass movements occurred while rivers were contacting terrace bluffs indicates that lateral fluvial erosion is usually necessary to prime terraces for failure. This supports our Hypothesis 2a and corroborates past inferences that fluvial oversteepening is necessary to generate terrace mass movements (LaHusen et al., 2016). However, the lack of correlation between the proportion of the stream network in contact with bluffs or valley bottom geometry and eroded volume or terrace mass movement frequency indicates that although lateral fluvial erosion is likely necessary to oversteepen bluff faces and trigger mass movements, it is insufficient alone to regulate their volume. This lack of correlation fails to support our Hypothesis 2b and indicates that the frequency and magnitude of terrace erosion may be better explained by hillslope geometry, material properties, and hydrology. Levees and revetments that restrict fluvial lateral erosion may prevent mass movements, especially those along outer bends. However, terraces have been primed for failure from fluvial erosion over thousands of years, and human alterations to rivers are likely not widespread enough spatially or temporally to significantly reduce long-term terrace sediment flux to Puget Sound rivers, despite perhaps reducing mass movement incidence in some areas.

The weak correlation between the proportion of Ql and terrace erosion volume in our data marginally supports our Hypothesis 3. A more comprehensive stratigraphic investigation of the mass movements we mapped is needed to test this hypothesis robustly, as the well log data used here involve large uncertainties and were available for only a few dozen mass movements. We also note that the multiple, discrete Ql layers we observed in many terraces present a more complicated stratigraphy than the conceptual stratigraphy modeled by Perkins et al. (2017). The relevance and influence of this more complicated stratigraphy is poorly understood. Ql may play a dominant role only in large, infrequent mass movements, only one of which was included in our study's short timeframe. Other processes and characteristics that we were unable to measure, such as groundwater hydrology, hillslope vegetation cover, and climatic factors may regulate terrace erosion magnitude and would be reasonable subjects for further investigation of the hillslope-specific controls on terrace sediment delivery as well as the controls on variability in terrace sediment delivery between basins.

### 4.3 Implications for Managing Terrace Mass Movements and Sediment Delivery in Puget Sound Watersheds

Terrace sediment delivery is an important sediment source to Puget Sound rivers. Especially for currently unglaciated basins such as the Stillaguamish, Snohomish, Cedar, Green, and Deschutes, management of sediment dynamics and estimates of sediment supply should consider terraces as potentially important sediment sources, particularly for downstream, lowland reaches. However, mass movement style, volume, and sedimentology vary substantially among individual terrace mass movements; this implies that efforts to manage terrace-derived

sedimentation would be well-served by site-specific evaluations of terrace sedimentology, the flux of sediment from terraces to rivers, and routing to lowland depositional reaches, as opposed to relying on regional estimates. Effective evaluation of terrace mass movement hazard should likewise focus on determining the site-specific sedimentologic characteristics, failure mechanisms, and failure frequency, especially due to the substantial variability in fluvial and hillslope processes that result in these failures. Efforts to stabilize terrace mass movements by restricting lateral migration may work for outer bend falls and outer bend lateral retreats, but terrace bluffs are inherently unstable and can fail even without fluvial erosion at their bases. While we show correlations between failure style and mass movement volume, more investigation is needed to determine the processes that determine failure mechanism and the probability of terrace mass movements.

The indication that fluvial lateral erosion likely primes terrace faces for failure in many cases suggests that high-sediment-transport-capacity floods may also result in substantial sediment delivery from terraces. This coincidence of sediment supply and transport implies that sediment currently stored adjacent to rivers in terraces is generally directly fluvially available, and further reinforces the need for detailed, basin-specific investigations of terrace sediment delivery to inform the management of sedimentation influences on issues such as flood hazard, levee and revetment evaluation, and restoration for rivers in Puget Sound and other regions having a similar paraglacial or paravolcanic sediment source.

## 5 Conclusions

Erosion of Pleistocene glacial and Holocene lahar terraces is a substantial sediment source to Puget Sound rivers. Moreover, this sediment source is dominated by small, frequent landslides, as opposed to large, infrequent landslides such as the 2014 Oso landslide. As a voluminous source of laterally connected, coarse, and resistant sediment low in river networks, these terraces may be especially important in regulating channel morphodynamics in lowland, depositional reaches. The variability in terrace sediment delivery among basins motivates more detailed characterizations of terrace stratigraphy and sediment size, as well as more explicit comparison of terrace erosion to other basin sediment sources, to quantifying the importance of terrace sediment to channels in lowland depositional reaches.

Terrace sediment delivery flux is a complex function of both short-term fluvial erosion and hillslope characteristics conditioned by longer-term fluvial erosion and past glacial and volcanic sediment deposition. While rivers can initiate terrace mass movements, valley bottom geometry poorly predicts mass movement volume. However, the geometry of the hillslopes on which these mass movements occur, likely set by long-term fluvial incision and terrace stratigraphy, correlates with failure mechanism and resulting terrace erosion volume. The roles of hillslope sedimentology and hydrology are good candidates for future study of the mechanistic controls on terrace mass movement volume and frequency. Because terrace mass movements result from a combination of fluvial and hillslope processes, unlike mass movements in environments not directly conditioned by fluvial processes, future development of our understanding of river-adjacent terrace mass movements must acknowledge the simultaneous importance of both fluvial and hillslope processes in regulating terrace mass movement volume and occurrence.

## 6 Acknowledgements

We thank Scott Anderson, Allison Pfeiffer, Shelby Ahrendt, Erkan Istanbulluoglu, Jacob Morgan, David Montgomery, Christina Bandaragoda, Nirnimesh Kumar, Jeffrey Keck, and Alex Horner-Devine for discussion that helped shape the ideas presented here. We thank Sean LaHusen, John Pitlick, and an anonymous reviewer for constructive comments that improved this manuscript. This work was funded by NSF PREEVENTS award 1663859.

## 7 Data Availability Statement

Data supporting the analyses presented here can be found in Dataset S1 (data organized by mass movement) and Dataset S2 (data organized by basin) and on EarthArxiv (https://eartharxiv.org/3mkzv/).

## 8 References


Aho, K., 2019. asbio: A Collection of Statistical Tools for Biologists.

Anderson, S., Konrad, C.P., Grossman, E.E., Curran, C.A., 2019. Sediment Storage and Transport in the Nooksack River Basin, Northwestern Washington, 2006–15 (Scientific Investigations Report No. 2019–5008). U.S. Geological Survey.

Anderson, S.W., Curran, C.A., Grossman, E.E., 2017. Suspended-sediment loads in the lower Stillaguamish River, Snohomish County, Washington, 2014–15 (Open-File Report No. 2017–1066), Open-File Report. U.S. Geological Survey.

Anderson, S.W., Jaeger, K.L., 2020. Coarse sediment dynamics in a large glaciated river system: Holocene history and storage dynamics dictate contemporary climate sensitivity. GSA Bulletin. https://doi.org/10.1130/B35530.1

Anderson, S.W., Konrad, C.P., 2019. Downstream-Propagating Channel Responses to Decadal-Scale Climate Variability in a Glaciated River Basin. Journal of Geophysical Research: Earth Surface 2018JF004734. https://doi.org/10.1029/2018JF004734

Armstrong, J.E., Crandell, D.R., Easterbrook, Donald J., Noble, J.B., 1965. Late Pleistocene Stratigraphy and Chronology in Southwestern British Columbia and Northwestern Washington. Geological Society of America Bulletin 76, 321–330.

Ballantyne, C.K., 2002. A general model of paraglacial landscape response. The Holocene 12, 371–376. https://doi.org/10.1191/0959683602hl553fa

Beechie, T.J., Collins, B.D., Pess, G.R., 2001. Holocene and recent geomorphic processes, land use, and salmonid habitat in two north Puget Sound river basins, in: Dorava, J.M., Montgomery, D.R., Palcsak, B.B., Fitzpatrick, F.A. (Eds.), Water Science and Application. American Geophysical Union, Washington, D. C., pp. 37–54. https://doi.org/10.1029/WS004p0037

Benda, L., Beechie, T.J., Wissmar, R.C., Johnson, A., 1992. Morphology and Evolution of Salmonid Habitats in a Recently Deglaciated River Basin, Washington State, USA. Canadian Journal of Fisheries and Aquatic Sciences 49, 1246–1256. https://doi.org/10.1139/f92-140

Bishara, A.J., Hittner, J.B., 2017. Confidence intervals for correlations when data are not normal. Behavior Research Methods 49, 294–309. https://doi.org/10.3758/s13428-016-0702-8

Booth, A.M., LaHusen, S.R., Duvall, A.R., Montgomery, D.R., 2017. Holocene history of deep-seated landsliding in the North Fork Stillaguamish River valley from surface roughness analysis, radiocarbon dating, and numerical landscape evolution modeling: Landsliding in the N. Fork Stillaguamish. Journal of Geophysical Research: Earth Surface 122, 456–472. https://doi.org/10.1002/2016JF003934

Booth, D.B., 1994. Glaciofluvial infilling and scour of the Puget Lowland, Washington, during ice-sheet glaciation. Geology 22, 695–698.

Church, M., Ryder, J.M., 1972. Paraglacial Sedimentation A Consideration of Fluvial Processes Conditioned by Glaciation. Geological Society of America Bulletin 83, 3059–3072.

Church, M., Slaymaker, O., 1989. Disequilibrium of Holocene sediment yield in glaciated British Columbia. Nature 337, 452–454.

Collins, B.D., Dickerson-Lange, S.E., Schanz, S., Harrington, S., 2019. Differentiating the effects of logging, river engineering, and hydropower dams on flooding in the Skokomish River, Washington, USA. Geomorphology 332, 138–156. https://doi.org/10.1016/j.geomorph.2019.01.021

Collins, B.D., Dunne, T., 1989. Gravel Transport, Gravel Harvesting, and Channel-Bed Degradation in Rivers Draining the Southern Olympic Mountains, Washington, U.S.A. Environ. Geol. Water Sci 13, 213–224. https://doi.org/10.1007/BF01665371

Collins, B.D., Montgomery, D.R., 2011. The legacy of Pleistocene glaciation and the organization of lowland alluvial process domains in the Puget Sound region. Geomorphology 126, 174–185. https://doi.org/10.1016/j.geomorph.2010.11.002

Crandell, D.R., 1971. Postglacial Lahars From Mount Rainier Volcano, Washington (Geological Survey Professional Paper No. 677). Washington, D. C.

Curran, C.A., Grossman, E.E., Magirl, C.S., Foreman, J.R., 2016a. Suspended sediment delivery to Puget Sound from the lower Nisqually River, western Washington, July 2010–November 2011 (Scientific Investigations Report No. 2016–5062), Scientific Investigations Report. U.S. Geological Survey.

Curran, C.A., Grossman, E.E., Mastin, M.C., Huffman, R.L., 2016b. Sediment load and distribution in the lower Skagit River, Skagit County, Washington (Scientific Investigations Report No. 2016–5106), Scientific Investigations Report. U.S. Geological Survey.

Czuba, J.A., Magirl, C.S., Czuba, C.R., Curran, C.A., Johnson, K.H., Olsen, T.D., Kimball, H.K., Gish, C.C., 2012. Geomorphic analysis of the river response to sedimentation downstream of Mount Rainier, Washington (Open-File Report No. 2012–1242), Open-File Report. U.S. Geological Survey.

Dethier, D.P., Pessl, F., Keuler, R.F., Balzarini, M.A., Pevear, D.R., 1995. Late Wisconsinan glaciomarine deposition and isostatic rebound, northern Puget Lowland, Washington. Geological Society of America Bulletin 107, 1288–1303.

Dragovich, J.D., Gilbertson, L.A., Lingley, Jr., W.S., Polenz, M., Glenn, J., 2002a. Geologic map of the Darrington 7.5-minute quadrangle, Skagit and Snohomish Counties, Washington (Open File Report No. 2002–7). Washington State Department of Natural Resources Division of Geology and Earth Resources.

Dragovich, J.D., Gilbertson, L.A., Lingley, Jr., W.S., Polenz, M., Glenn, J., 2002b. Geologic map of the Fortson 7.5-minute quadrangle, Skagit and Snohomish Counties, Washington (Open File Report No. 2002–6). Washington State Department of Natural Resources Division of Geology and Earth Resources.

Fox, J., Weisberg, S., 2019. An {R} Companion to Applied Regression, 3rd ed. Sage, Thousand Oaks, CA.

Gardner, B., Loewus-Deitch, J., Emerick, C., DeBari, M., Slattery, K., 2009. State Route 542: Warnick Bluff Stabilization: WSDOT-Identified Chronic Environmental Deficiencies Mitigation to Protect Infrastructure and Reduce Potential Environmental Damage (Huxley College Graduate and Undergraduate Publications). Western Washington University.

Gomez, C., Lavigne, F., 2010. Transverse architecture of lahar terraces, inferred from radargrams: preliminary results from Semeru Volcano, Indonesia. Earth Surf. Process. Landforms 35, 1116–1121. https://doi.org/10.1002/esp.2016

Gran, K.B., Finnegan, N., Johnson, A.L., Belmont, P., Wittkop, C., Rittenour, T., 2013. Landscape evolution, valley excavation, and terrace development following abrupt postglacial base-level fall. Geological Society of America Bulletin 125, 1851–1864. https://doi.org/10.1130/B30772.1

Hungr, O., Leroueil, S., Picarelli, L., 2014. The Varnes classification of landslide types, an update. Landslides 11, 167–194. https://doi.org/10.1007/s10346-013-0436-y

Iverson, R.M., George, D.L., Allstadt, K., Reid, M.E., Collins, B.D., Vallance, J.W., Schilling, S.P., Godt, J.W., Cannon, C.M., Magirl, C.S., Baum, R.L., Coe, J.A., Schulz, W.H., Bower, J.B., 2015. Landslide mobility and hazards: implications of the 2014 Oso disaster. Earth and Planetary Science Letters 412, 197–208. https://doi.org/10.1016/j.epsl.2014.12.020

Kessler, A.C., Gupta, S.C., Brown, M.K., 2013. Assessment of river bank erosion in Southern Minnesota rivers post European settlement. Geomorphology 201, 312–322. https://doi.org/10.1016/j.geomorph.2013.07.006

King County, 2020. Levees and revetments, King County, Washington [WWW Document]. URL https://www.kingcounty.gov/depts/dnrp/wlr/sections-programs/river-floodplain-section/maintenance.aspx (accessed 2.14.20).

King County, 2018. Field Report and Preliminary Analysis, 7/10/2018 Site Visit to Landslide on Palmer Mountain along South Fork Skykomish River, River Mile 9.3. Prepared by Judi Radloff and Jeremy Bunn. King County Water and Land Resources Division Department of Natural Resources and Parks, Seattle, WA.

Klösch, M., Blamauer, B., Habersack, H., 2015. Intra-event scale bar-bank interactions and their role in channel widening. Earth Surf. Process. Landforms 40, 1506–1523. https://doi.org/10.1002/esp.3732

Kovanen, D., Slaymaker, O., 2015. The paraglacial geomorphology of the Fraser Lowland, southwest British Columbia and northwest Washington. Geomorphology 232, 78–93. https://doi.org/10.1016/j.geomorph.2014.12.021

LaHusen, S.R., Duvall, A.R., Booth, A.M., Montgomery, D.R., 2016. Surface roughness dating of long-runout landslides near Oso, Washington (USA), reveals persistent postglacial hillslope instability. Geology 44, 111–114. https://doi.org/10.1130/G37267.1

Millard, S.P., 2013. EnvStats: An R Package for Environmental Statistics. Springer, New York.

Nelson, L.M., 1974. Sediment transport by streams in the Deschutes and Nisqually River Basins, Washington, November 1971 - June 1973 (Open-File Report). United States Department of the Interior Geological Survey, Tacoma, Washington.

Nelson, L.M., 1971. Sediment Transport by Streams in the Snohomish River Basin, Washington October 1967 - June 1969. United States Department of the Interior Geological Survey Water Resources Division, Tacoma, Washington.

Northwest Hydraulic Consultants, Inc., 2018. Cedar River 2018 Annual Sediment Report. City of Renton, Renton, WA.

O'Connor, J.E., Mangano, J.F., Anderson, S.W., Wallick, J.R., Jones, K.L., Keith, M.K., 2014. Geologic and physiographic controls on bed-material yield, transport, and channel morphology for alluvial and bedrock rivers, western Oregon. Geological Society of America Bulletin 126, 377–397. https://doi.org/10.1130/B30831.1

Perkins Geosciences, Harper Houf Righellis, Inc., 2002. Cedar River Gravel Study Phase 2 Report.

Perkins, J.P., Reid, M.E., Schmidt, K.M., 2017. Control of landslide volume and hazard by glacial stratigraphic architecture, northwest Washington State, USA. Geology 45, 1139–1142. https://doi.org/10.1130/G39691.1

Powers, P.D., Helstab, M., Niezgoda, S.L., 2019. A process-based approach to restoring depositional river valleys to Stage 0, an anastomosing channel network. River Research and Applications 35, 3–13. https://doi.org/10.1002/rra.3378

PRISM Climate Group, Oregon State University, 2012. 30-yr Normal Precipitation: Annual, Period 1981-2010.

R Core Team, 2018. R: A language and environment for statistical computing. R Foundation for Statistical Computing, Vienna, Austria.

Roux, C., Alber, A., Bertrand, M., Vaudor, L., Piégay, H., 2015. "FluvialCorridor": A new ArcGIS toolbox package for multiscale riverscape exploration. Geomorphology 242, 29–37. https://doi.org/10.1016/j.geomorph.2014.04.018

RStudio Team, 2016. RStudio: Integrated Development Environment for R. RStudio, Inc., Boston, MA.

Savage, W.Z., Morrissey, M.M., Baum, R.L., 2000. Geotechnical Properties for Landslide-Prone Seattle Area Glacial Deposits (Open-File Report No. 00–228), Open-File Report. U.S. Geological Survey, Denver, CO.

Schumm, S.A., 1977. The fluvial system. Wiley, New York.

Scott, K.M., Tucker, D.S., Riedel, J.L., Gardner, C.A., McGeehin, J.P., 2020. Latest Pleistocene to Present Geology of Mount Baker Volcano, Northern Cascade Range, Washington: U.S. Geological Survey Professional Paper 1865 (Professional Paper), Professional Paper.

Senter, C.A., Conn, K.E., Black, R.W., Peterson, N., Vanderpool-Kimura, A., Foreman, J.R., 2018. Suspended-sediment transport from the Green-Duwamish River to the Lower Duwamish Waterway, Seattle, Washington, 2013–17 (Open-File Report No. 2018–1029), Open-File Report. U.S. Geological Survey.

Slaymaker, O., 2009. Proglacial, periglacial or paraglacial? Geological Society, London, Special Publications 320, 71–84. https://doi.org/10.1144/SP320.6

Slaymaker, O., 2003. The sediment budget as conceptual framework and management tool. Hydrobiologia 494, 71–82. https://doi.org/10.1023/A:1025437509525

Stover, S.C., Montgomery, D.R., 2001. Channel change and flooding, Skokomish River, Washington. Journal of Hydrology 15.

Thorson, R.M., 1980. Ice-Sheet Glaciation of the Puget Lowland, Washington, during the Vashon Stade (Late Pleistocene). Quaternary Research 13, 303–321. https://doi.org/10.1016/0033-5894(80)90059-9

Troost, K.G., 2016. Chronology, Lithology and Paleoenvironmental Interpretations of the Penultimate Ice-Sheet Advance into the Puget Lowland, Washington State (Dissertation). University of Washington, Seattle, WA.

United States Army Corp of Engineers, 2020. Levees of the Nation [WWW Document]. URL https://levees.sec.usace.army.mil/#/ (accessed 2.26.20).

Vallance, J.W., Scott, K.M., 1997. The Osceola Mudflow from Mount Rainier: Sedimentology and hazard implications of a huge clay-rich debris flow. Geological Society of America Bulletin 21.

Varnes, D.J., 1958. Landslide Types and Processes. Landslides and engineering practice 24, 20–47.

Wartman, J., Montgomery, D.R., Anderson, S.A., Keaton, J.R., Benoît, J., dela Chapelle, J., Gilbert, R., 2016. The 22 March 2014 Oso landslide, Washington, USA. Geomorphology 253, 275–288. https://doi.org/10.1016/j.geomorph.2015.10.022

Washington Division of Geology and Earth Resources, 2016. Surface Geology 100k Geodatabase (Washington Division of Geology and Earth Resources Digital Data Series No. DS-18, version 3.1).

Washington State Department of Ecology, 2020. Washington State Well Report Viewer [WWW Document]. URL https://appswr.ecology.wa.gov/wellconstruction/map/WCLSWebMap/default.aspx (accessed 1.15.20).

Wickham, H., 2016. ggplot2: Elegant Graphics for Data Analysis. Springer-Verlag, New York.

Wickham, H., Averick, M., Bryan, J., Chang, W., McGowan, L., François, R., Grolemund, G., Hayes, A., Henry, L., Hester, J., Kuhn, M., Pedersen, T., Miller, E., Bache, S., Müller, K., Ooms, J., Robinson, D., Seidel, D., Spinu, V., Takahashi, K., Vaughan, D., Wilke, C., Woo, K., Yutani, H., 2019. Welcome to the Tidyverse. JOSS 4, 1686. https://doi.org/10.21105/joss.01686

Wilke, C.O., 2019. cowplot: Streamlined Plot Theme and Plot Annotations for "ggplot2."

Wohl, E., 2020. Rivers in the Landscape, 2nd ed. John Wiley & Sons Ltd, Oxford, UK.

Wohl, E., Brierley, G., Cadol, D., Coulthard, T.J., Covino, T., Fryirs, K.A., Grant, G., Hilton, R.G., Lane, S.N., Magilligan, F.J., Meitzen, K.M., Passalacqua, P., Poeppl, R.E., Rathburn, S.L., Sklar, L.S., 2019. Connectivity as an emergent property of geomorphic systems: Geomorphic connectivity. Earth Surface Processes and Landforms 44, 4–26. https://doi.org/10.1002/esp.4434